Transverse Mode with Y-Junction Structures in Broad-Area Oxide-Confined Vertical-Cavity Surface-Emitting Laser

2003 Jpn. J. Appl. Phys. 42 L458

(http://iopscience.iop.org/1347-4065/42/5A/L458)

Jpn. J. Appl. Phys. Vol. 42 (2003) pp. L458–L460
Part 2, No. 5A, 1 May 2003

Transverse Mode with Y-Junction Structures in Broad-Area Oxide-Confined Vertical-Cavity Surface-Emitting Laser

Ren-Jay Kou* and Ci-Ling Pan

Institute of Electro-Optical Engineering, National Chiao-Tung University, Hsinchu, Taiwan 300, Republic of China

(Received December 26, 2002; accepted for publication March 5, 2003)

We present experimental data characterizing the first-observed transverse mode with *y*-junction structures in a broad-area (20 µm in diameter) oxide-confined vertical-cavity surface-emitting laser at a 22.3 mA injection current which is larger than the thermal roll-over point. The formation of the *y*-junction structured pattern, which can be observed in far-field images, is due to an interaction between adjacent high-order transverse modes. [DOI: 10.1143/JJAP.42.L458]

KEYWORDS: *y*-junction, high-order transverse mode, broad-area oxide-confined vertical-cavity surface-emitting lasers

The vertical-cavity surface-emitting laser (VCSEL) is a well-established device for applications in optical communications, optical interconnections, optical neural networks, and optical signal processing. However, because of the possibility of a large Fresnel number,[1] a rich variety of mode dynamics can therefore be expected in oxide-confined VCSEL such as the whispering gallery modes,[2,3] Hermite-Gaussian, Laguerre-Gaussian modes,[4–7] and others.[8–10]

In this study, we observe the transverse modes with *y*-junction structures in a broad-area oxide-confined VCSEL while the injection current is larger than the thermal roll-over point. We experimentally investigate the near- and far-field transverse modes and corresponding spectral data under a CW pumping condition. Due to the inhomogeneous distribution of carriers and temperature in conjunction with a large index step supported by the oxidized layers, the VCSEL under investigation is operated in a multi transverse high-order-mode regime. The interaction between these high-order transverse modes causes the formation of a complex *y*-junction structured pattern which can only be observed in far-field images.

The device under investigation is a broad-area (20 µm in diameter) oxide-confined VCSEL grown using metal-organic chemical vapor deposition (MOCVD) to emit at approximately 809 nm. Its active region comprises three $Al_{0.08}Ga_{0.92}As$–$Al_{0.36}Ga_{0.64}As$ quantum wells clad in spacers to form a single-wavelength-long cavity. A high-Al composition $Al_{0.97}Ga_{0.03}As$ layer placed at the first p-type doping distributed Bragg reflector (p-DBR) mirror is oxidized for current and optical confinement. The optical power versus injection current characteristic of oxide-confined VCSEL is shown in Fig. 1, which reveals significant thermal roll-over behavior. Its threshold current is ~2.7 mA and its maximum power is ~6.4 mW. To study its characteristics of spatial distribution, we couple the near-field image onto the beam profiler using a collimating objective lens. As for far-field image, we project the far-field pattern on a screen and then record it with a CCD camera.

Near-field images of the 20 µm diameter oxide-confined VCSEL are presented in Fig. 2, and corresponding spectrum is shown in Fig. 3. A noncircular symmetry of the transverse mode can be already seen from a first look at the optical near-field images because of the anisotropic oxidation speed.[7] While the injection current is 22.3 mA, which is larger than the thermal roll-over point, the high-intensity

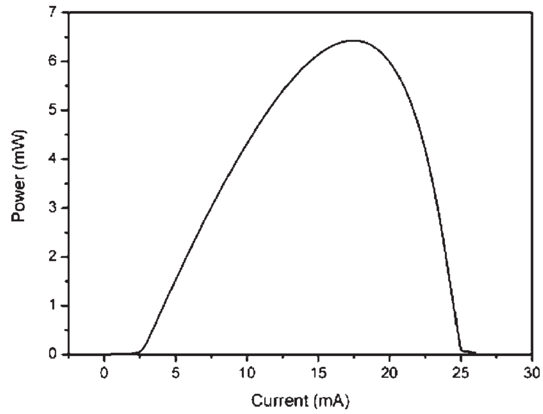

Fig. 1. Light output vs current curve of 20 µm diameter oxidized VCSEL under CW operation at room temperature.

distribution can only be observed around the periphery of the oxide aperture as shown in Fig. 2(a). The laser is operated in multi transverse modes according to the corresponding spectrum in Fig. 3(a). These two results indicate that the multiple high-order transverse modes tend to gather around the periphery of the oxide aperture due to a strong optical confinement induced by the oxidized layers. Therefore the *y*-junction structured pattern cannot be observed in the near-field images. At an even larger injection current of 23.3 mA, the lasing near-field pattern becomes a pure single high-order mode which has 18 spots as shown in Figs. 2(b) and 3(b). The results reveal that the mode suppression is strongly influenced by thermal effect, and the inhomogeneous distributions of spatial carriers and thermal gradients in the laser cause a strong tendency towards the emission of high-order transverse modes.[4]

We present the far-field intensity distribution in Fig. 4, which contains the 180°-rotation symmetrical images at injection currents of 22.3 mA (a) and 23.3 mA (b). The *y*-junction structured pattern is observed in Fig. 4(a) and a 9th-order daisy mode is observed in Fig. 4(b). Since the lasing modes of the VCSEL at 22.3 mA are multiple transverse modes according to Fig. 3(a) and these high-order transverse modes have similar divergent angles in far-field emission as shown in Fig. 4(a), we conclude that the interaction between the adjacent high-order transverse modes induces the formation of the *y*-junction structured pattern.

The *y*-junction structured pattern is extensively observed in studies of pattern formation.[11–13] One of the complex

*E-mail address: rjkou.eo85g@nctu.edu.tw

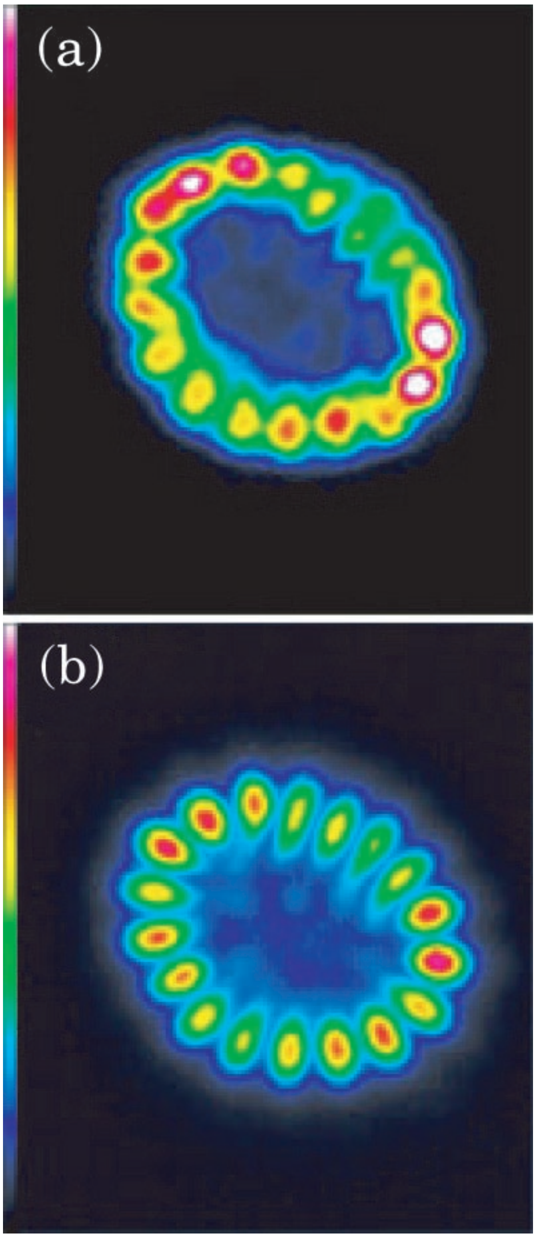

Fig. 2. Photographs of near-field patterns of 20 μm diameter oxide-confined VCSEL at injection currents of (a) 22.3 mA and (b) 23.3 mA.

dynamics that govern these patterns is perhaps the occurrence of instabilities and symmetry breaking. In lasers, the *y*-junction structured pattern observed so far was in the interferogram of optical vortices.[14,15] The interference fringe with *y*-junction structured pattern is called "edge phase dislocation"[14] or "forks".[15] For the broad-area oxide-confined VCSEL, the *y*-junction structured pattern in far-field intensity distribution is first reported. The *y*-junction structured pattern is observed in the far-field emission pattern while the injection current is 22.3 mA, which is larger than the thermal roll-over point. With an even larger current, the thermal effect dominates, and the far-field emission pattern becomes a 9th-order daisy mode due to inhomogeneous distributions of carriers and thermal gradients.

In conclusion, we have presented experimental data of the transverse lasing modes with *y*-junction structure in a broad-area (20 μm in diameter) oxide-confined VCSEL at an

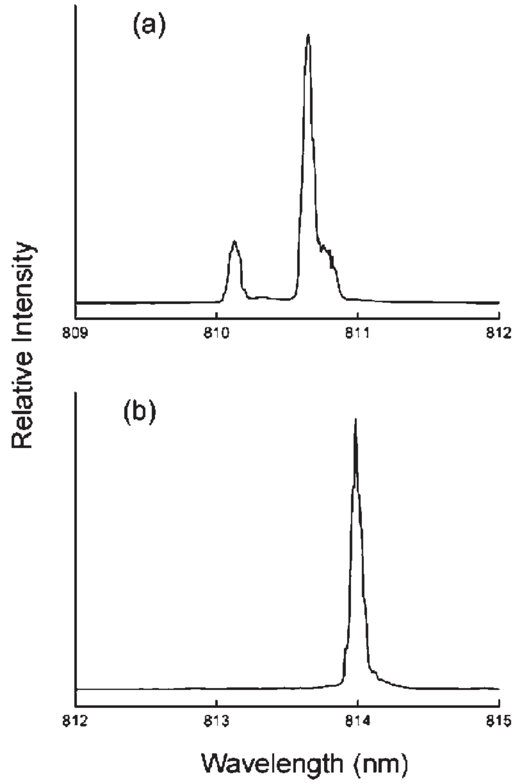

Fig. 3. Spectral data of 20 μm diameter oxide-confined VCSEL at injection currents of (a) 22.3 mA and (b) 23.3 mA.

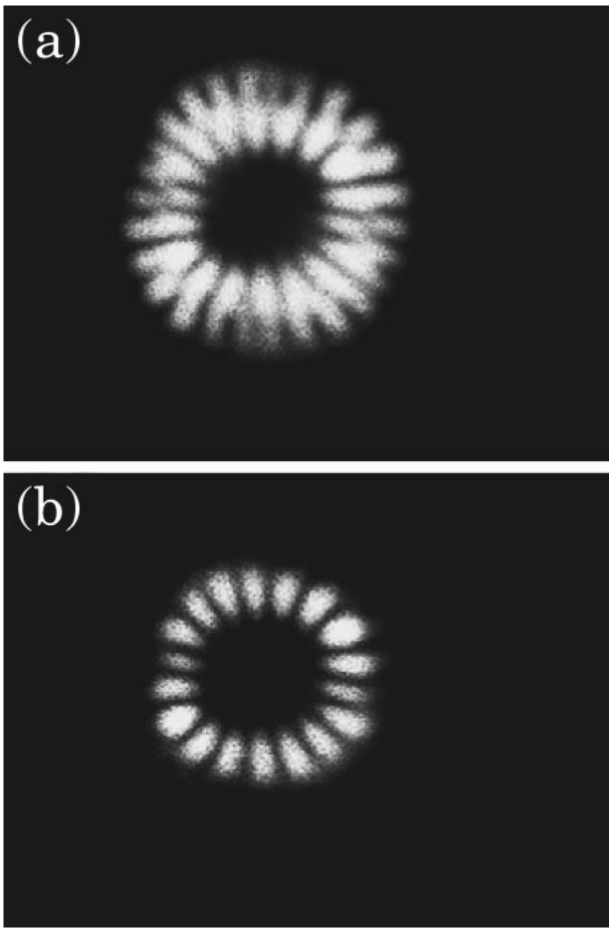

Fig. 4. Photographs of far-field patterns of 20 μm diameter oxide-confined VCSEL at injection currents of (a) 22.3 mA and (b) 23.3 mA.

injection current which is larger than the thermal roll-over point. In near-field experimental results, a strong optical confinement introduced by the oxidized layers causes the multiple high-order transverse modes to gather around the periphery of the oxide aperture so that the *y*-junction structured pattern cannot be observed. Based on the far-field experimental results, we conclude that these adjacent high-order transverse modes with similar divergent angles induce an interaction which causes the formation of the *y*-junction structures.

The authors would like to thank Dr. J. S. Pan, H. C. Lai, and M. C. Tang at TrueLight Corp. for the assistance of oxidized VCSEL manufacturing; Assistant Professor Y. F. Chen and Ph. D. student Y. P. Lan at National Chiao-Tung University for the optical measurement and discussions.

1) S. P. Hegarty, G. Huyet, J. G. McInerney and K. D. Choquette: Phys. Rev. Lett. **82** (1999) 1434.
2) H. Deng, Q. Deng and D. G. Deppe: Appl. Phys. Lett. **69** (1996) 3120.
3) Q. Deng, H. Deng and D. G. Deppe: Opt. Lett. **22** (1997) 463.
4) C. Degen, I. Fischer and W. Elsasser: Opt. Exp. **5** (1999) 38.
5) C. Degen, B. Krauskopf, G. Jennemann, I. Fischer and W. Elsasser: J. Opt. B: Quantum & Semiclassical Opt. **2** (2000) 517.
6) C. Degen, I. Fischer, W. Elsasser, L. Fratta, P. Debernardi, G. P. Bava, M. Brunner, R. Hovel, M. Moser and K. Gulden: Phys. Rev. A **63** (2001) 023817.
7) P. Debernardi, G. P. Bava, C. Degen, I. Fischer and W. Elsasser: IEEE J. Quantum Electron. **38** (2002) 73.
8) D. L. Huffaker, H. Deng, Q. Deng and D. G. Deppe: Appl. Phys. Lett. **69** (1996) 3477.
9) S. P. Hegarty, G. Huyet, P. Porta, J. G. McInerney, K. D. Choquette, K. M. Geib and H. Q. Hou: J. Opt. Soc. Am. B **16** (1999) 2060.
10) T. Ackemann, S. Barland, M. Cara, S. Balle, J. R. Tredicce, R. Jager, M. Grabherr, M. Miller and K. J. Ebeling: J. Opt. B: Quantum & Semiclassical Opt. **2** (2000) 406.
11) S. Ciliberto, E. Pampaloni and C. Perez-Garcia: Phys. Rev. Lett. **61** (1988) 1198.
12) S. Kondo and R. Asai: Nature **376** (1995) 765.
13) H. Meinhardt: Nature **376** (1995) 722.
14) D. V. Petrov: Opt. & Quantum Electron. **34** (2002) 759.
15) C. O. Weiss, M. Vaupel, K. Staliunas, G. Slekys and V. B. Taranenko: Appl. Phys. B: Lasers & Opt. B **68** (1999) 151.